

On the Curie temperature dependency of the magnetocaloric effect

J. H. Belo, J. S. Amaral, A. M. Pereira, V. S. Amaral, and J. P. Araújo

Citation: *Appl. Phys. Lett.* **100**, 242407 (2012); doi: 10.1063/1.4726110

View online: <http://dx.doi.org/10.1063/1.4726110>

View Table of Contents: <http://apl.aip.org/resource/1/APPLAB/v100/i24>

Published by the [American Institute of Physics](#).

Related Articles

Controllable spin-glass behavior and large magnetocaloric effect in Gd-Ni-Al bulk metallic glasses
Appl. Phys. Lett. **101**, 032405 (2012)

History dependence of directly observed magnetocaloric effects in (Mn, Fe)As
Appl. Phys. Lett. **100**, 252409 (2012)

The magnetocaloric effect of partially crystalline Fe-B-Cr-Gd alloys
J. Appl. Phys. **111**, 113919 (2012)

Normal or inverse magnetocaloric effects at the transition between antiferromagnetism and ferromagnetism
Appl. Phys. Lett. **100**, 242408 (2012)

Spin reorientation and the magnetocaloric effect in $\text{Ho}_{1-y}\text{Er}_y\text{N}$
J. Appl. Phys. **111**, 113916 (2012)

Additional information on *Appl. Phys. Lett.*

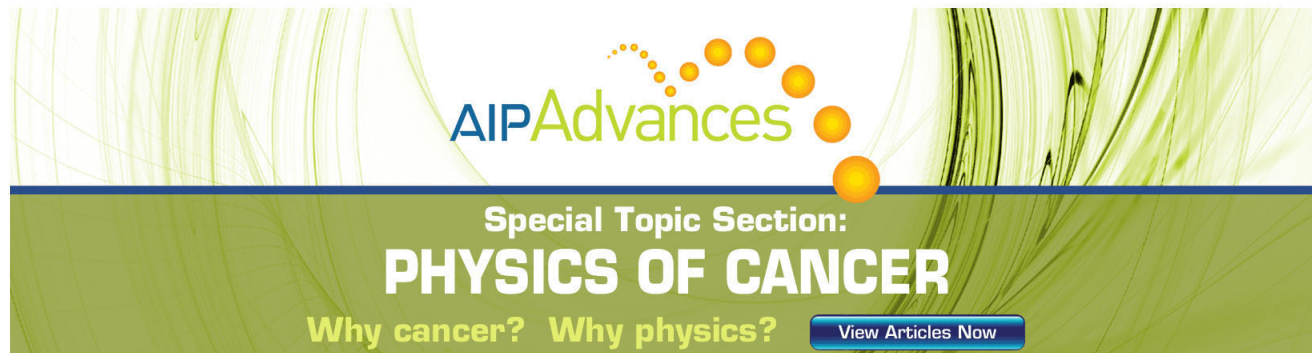
Journal Homepage: <http://apl.aip.org/>

Journal Information: http://apl.aip.org/about/about_the_journal

Top downloads: http://apl.aip.org/features/most_downloaded

Information for Authors: <http://apl.aip.org/authors>

ADVERTISEMENT

The advertisement features a green background with abstract, flowing lines. At the top, the 'AIP Advances' logo is shown, with 'AIP' in blue and 'Advances' in green, accompanied by a series of orange dots. Below the logo, the text 'Special Topic Section: PHYSICS OF CANCER' is displayed in white, with 'PHYSICS OF CANCER' in a larger, bold font. At the bottom, the phrase 'Why cancer? Why physics?' is written in yellow, and a blue button with the text 'View Articles Now' is positioned to the right.

AIP Advances

Special Topic Section:
PHYSICS OF CANCER

Why cancer? Why physics? [View Articles Now](#)

On the Curie temperature dependency of the magnetocaloric effect

J. H. Belo,¹ J. S. Amaral,^{1,2,a)} A. M. Pereira,¹ V. S. Amaral,² and J. P. Araújo^{1,b)}

¹IFIMUP and IN-Institute of Nanoscience and Nanotechnology, Departamento de Física e Astronomia da Faculdade de Ciências da Universidade do Porto, Rua do Campo Alegre, 687, 4169-007 Porto, Portugal

²Departamento de Física and CICECO, Universidade de Aveiro, 3810-193 Aveiro, Portugal

(Received 13 April 2012; accepted 18 May 2012; published online 13 June 2012; corrected 2 July 2012)

We investigate the magnetocaloric effect dependency on the most important microscopic parameters of ferromagnetic materials, such as the Curie temperature (T_C), the spin value (J), and the magnetic field change (ΔH). Second- and first-order phase transition systems are considered, using the Bean-Rodbell model [C. P. Bean and D. S. Rodbell, Phys. Rev. **126**, 104 (1962)] of magnetovolume interactions on the Weiss mean-field model [P. Weiss, J. Phys. Theory Appl. **6**, 661 (1907)]. The magnetocaloric effect simulations show a surprising $T_C^{-2/3}$ linear dependence of the maximum entropy change ($\Delta S_{m_{max}}$), which is observed for all simulated systems. An approximate state equation establishing the dependence of $\Delta S_{m_{max}}$ on T_C , ΔH , J , and the magnetic atoms density (N) is presented. The dependence of maximum magnetic entropy change on $T_C^{-2/3}$ is validated by a wide set of experimental results of second- and first-order phase transition materials that are promising for magnetic refrigeration applications at room temperature. © 2012 American Institute of Physics. [<http://dx.doi.org/10.1063/1.4726110>]

For the past fifteen years, since the discovery of the giant magnetocaloric effect (MCE) in the $R_5(\text{Si,Ge})_4$ system¹ near room temperature (RT), a very devoted effort has been made into the understanding of this phenomenon. The magnetic refrigeration near RT, which makes use of the MCE, possesses several eco-friendly features, namely, its high efficiency, absence of environmentally harmful gases, and low maintenance costs.²⁻⁴ Nevertheless, the magnetic refrigeration near RT still has not been able to compete with the conventional refrigeration technology. One of the major achievements to be accomplished is to find the most suitable magnetocaloric material in this temperature range. Namely, an intense debate on which kind of magnetic transitions (first or second order) are preferable for the RT magnetic refrigeration devices is still occurring nowadays.⁵⁻⁸ So far, the most promising compound families from the point of view of technological applications at RT include $R_5(\text{Si,Ge})_4$ (R is for Rare Earth), RM_2 (M is for Al, Co or Ni), $\text{MnFe}(\text{P}_{1-x}\text{As}_x)$, $\text{La}(\text{Fe}_{13-x}\text{Si}_x)$, and the manganites $\text{R}_{1-x}\text{M}_x\text{MnO}_3$ (M is for Ca, Sr and Ba). All these materials have been thoroughly characterized and their most important magnetic properties are known and are well reviewed in the following references.^{2-4,9,10} The most conventional way to characterize the MCE of a given magnetic material is through the temperature dependence of its magnetic entropy change ($\Delta S_m(T)$) for a given applied field change (ΔH), namely, through its peak value ($\Delta S_{m_{max}}$), Curie temperature (T_C), which establishes the optimal operating temperature, and the refrigerant capacity (product of full width at half maximum, $\text{FWHM}_{\Delta S_m(T)}$, and the $\Delta S_{m_{max}}$), which estimates the range of operating temperature. A considerable theoretical effort has been made on applying various models to the study of the MCE, from phenomenological theories¹¹⁻¹³ to microscopic models.¹⁴ Nevertheless, there is still a notable

lack of direct relations between the MCE and microscopic magnetic parameters, as recently evidenced in Ref. 15.

Herein, we have performed theoretical simulations to study the dependence of the $\Delta S_m(T)$ curves on the following parameters: Curie temperature (T_C), spin value (J), the applied magnetic field change (ΔH) for both first- and second-order magnetic transitions. The simulated $\Delta S_m(T)$ curves were obtained within the basis of the molecular mean field model,¹⁶ by solving numerically the following state equation for spin J :

$$M = NgJ\mu_B\mathcal{B}_J\left(\frac{Jg\mu_B H + \lambda(M)M}{k_B T}\right), \quad (1)$$

where M is magnetization, N is the density of magnetic atoms, g the g-factor, μ_B the Bohr magneton, \mathcal{B}_J is the Brillouin function for spin J , k_B is the Boltzmann constant, H the applied magnetic field, T the temperature, and λ the Weiss molecular mean-field exchange parameter. As was previously done,¹¹ it is possible to include the Bean Rodbell¹⁷ volume dependency of the exchange energy and in this way simulate first and second order magnetic transitions.

Fig. 1(a) shows the temperature dependencies of $\Delta S_m(T)$ normalized with the $Nk_B \ln(2J+1)$ factor (maximum entropy value) for a set of systems undergoing second order magnetic phase transitions in the 150–400 K temperature range. As can be seen in (a) a strong attenuation of the $\Delta S_{m_{max}}$ value with increasing T_C is observed. Contrarily, the FWHM increases significantly, i.e., a broadening of the $\Delta S_m(T)$ curves with increasing T_C is observed. This results from the fact that for a J value system the area under the $\Delta S_m(T)$ curve corresponds to the free energy change between a fully ordered state at $T \ll T_C$ and fully-disordered at $T \gg T_C$, which is independent on the T_C value itself. In order to study the dependence of the $\Delta S_{m_{max}}$ with the total spin number ($J = 1/2$, 2, and $7/2$) and with the applied magnetic field amplitude ($\Delta H = 1$ and 5 T),

^{a)}Electronic mail: jamaral@ua.pt.

^{b)}Electronic mail: jearaujo@fc.up.pt.

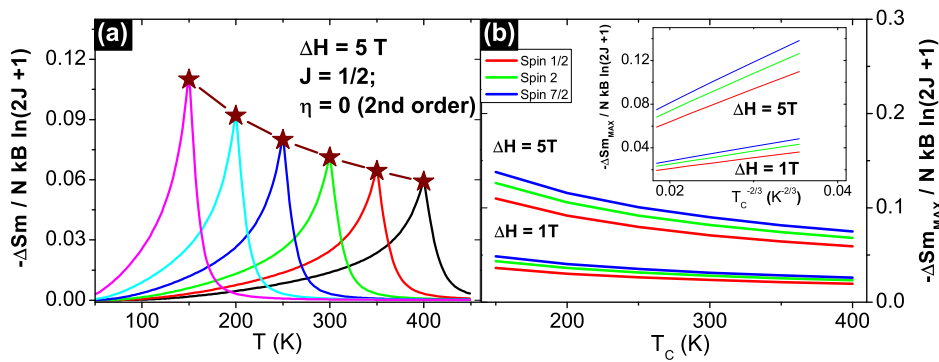


FIG. 1. (a) Temperature dependence of the normalized magnetic entropy change for a set of simulated systems with T_C in the range 150–400 K undergoing second order magnetic transitions. In (b) the dependence of the magnetic entropy change maxima on the Curie temperature for systems with different spin values and applied fields is plotted. In (b) inset, the $\Delta S_{m_{max}}$ is represented as a linear function of $T_C^{-2/3}$.

six different simulations were performed as shown in Fig. 1(b). As can be seen in this figure, the $\Delta S_{m_{max}}(T_C)$ curves show that there are no major changes in the overall behavior for different spins within the same applied field amplitude. Moreover, the $\Delta S_{m_{max}}$ values are higher for higher total spin number within the whole T_C range, as was expected. Furthermore, it is found that the effect of increasing the applied field change (from 1 to 5 T) enhances this difference between the obtained $\Delta S_{m_{max}}(T_C)$ curves for systems with different J . At the lowest Curie temperature, 150 K, and for $\Delta H = 5$ T, the $J = 7/2$ system achieves $\sim 14\%$ of its maximum theoretical entropy change, in contrast with only 11% for the $J = 1/2$ system. It is important to remark that here we are comparing relative $\Delta S_{m_{max}}$ values, since for all systems these values were normalized to their maximum theoretical value, $Nk_B \ln(2J+1)$. In the inset of Fig. 1(b), the $\Delta S_{m_{max}}$ values for the three different spin value systems with $\Delta H = 1$ and 5 T are represented as a function of $T_C^{-2/3}$. Although each spin value system presents a different slope, a striking linear dependence of $\Delta S_{m_{max}}$ on $T_C^{-2/3}$ is clearly observed.

In order to interpret and justify the $T_C^{-2/3}$ dependency of the $\Delta S_{m_{max}}$, we performed simple analytical derivations starting from the Weiss mean field equation of state, eq. (1). This equation is rearranged in the following form:

$$\frac{Jg\mu_B}{k_B} \frac{H + \lambda M}{T} = \mathcal{B}_J^{-1} \left(\frac{M}{Ng\mu_B J} \right), \quad (2)$$

where \mathcal{B}_J^{-1} represents the inverse Brillouin function for spin J .

Considering the Taylor expansion of the inverse Brillouin function,¹⁸ Eq. (2) can be approximated to the following equation of state:

$$\frac{H}{M} = \frac{1}{C}(T - T_C) + \frac{K}{C^2}TM^2 + \frac{K'}{C^3}TM^4 + \dots, \quad (3)$$

where

$$K = \frac{2J^2 + 2J + 1}{10J(J+1)k_B N}, \quad (4)$$

$$K' = \frac{44(2J+1)^2(J^2 + J + 1) - (2J+1)^2}{2800J^2(J+1)^2k_B^2 N^2}, \quad (5)$$

C the Curie constant,

$$C = \frac{NJ(J+1)g^2\mu_B^2}{3k_B}, \quad (6)$$

and $T_C = C \times \lambda$. Our description is for an arbitrary spin value. Nevertheless, for the particular case of a $J = 1/2$, the inverse Brillouin function is simply \tanh , while for $J = \infty$ and 4 , other approximate expressions are available.^{19,20}

By integrating on M , the free energy of the system is given

$$G = G_0 - MH + \frac{1}{2C}(T - T_C)M^2 + \frac{K}{4C^2}TM^4 + \frac{K'}{6C^3}TM^6 + \dots \quad (7)$$

Equation (7) shares the same structure in even powers of M as the typical Landau theory expansion of the free energy,^{12,21} however with an explicit linear dependence of the higher-order Landau parameters on T .

The state equation allows an analytic description of the field dependence of the MCE (ΔS_m) of a mean-field system, considering the temperature derivative of the free energy expression in Eq. (7)

$$-S_M = \frac{\partial G}{\partial T} = \frac{1}{2C}M^2 + \frac{K}{4C^2}M^4 + \frac{K'}{6C^3}M^6 + \dots \quad (8)$$

From the state equation, the field dependence of magnetization at $T = T_C$ (critical isotherm) is

$$M = \left(\frac{C^2}{K} \right)^{1/3} \left(\frac{H}{T_C} \right)^{1/3} + \dots \quad (9)$$

The magnetic entropy change due to a field change from 0 to H at $T = T_C$ ($\Delta S_m^{T=T_C} = \Delta S_{m_{max}}$) is then

$$-\Delta S_{m_{max}} = \frac{1}{2C} \left(\frac{C^2}{K} \right)^{2/3} \left(\frac{H}{T_C} \right)^{2/3} + \dots \quad (10)$$

Equation (10) justifies the $T_C^{-2/3}$ dependency of $\Delta S_{m_{max}}$ found in our second order systems simulations. It is important to stress that Eq. (10) also allows to relate $\Delta S_{m_{max}}$ with known parameters of these analytic ferromagnetic systems, such as N , J , and the applied magnetic field H (in a field change from 0 to H). From Eq. (10), it is obvious that these parameters values define the slope of the curve $\Delta S_{m_{max}}(T_C^{-2/3})$, hence explaining the different slopes obtained for $J = 1/2$, 2 , and $7/2$ and for the different applied field changes within the same spin number, as is seen in Fig. 1(b) inset. In fact, the ratios between the two slopes (one for $\Delta H = 1$ and

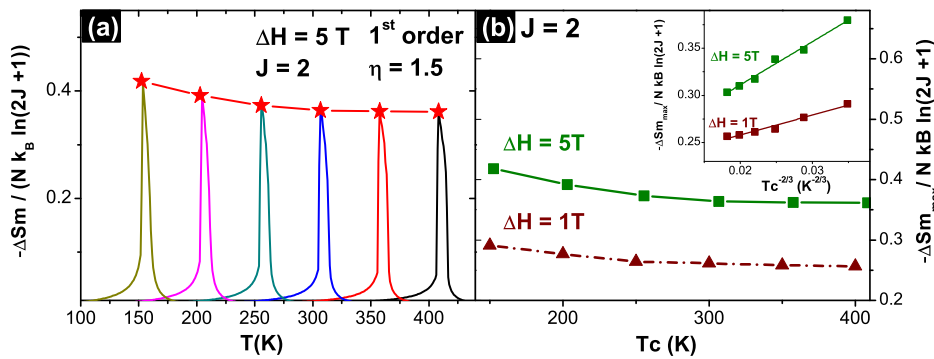


FIG. 2. (a) Temperature dependence of the magnetic entropy change (normalized) for a set of simulated systems undergoing first-order magnetic transitions ($\eta = 1.5$) with different T_C . In (b) the dependency of the entropy change maxima (ΔS_{max}) on the T_C for two different applied magnetic fields ($\Delta H = 1$ and 5 T) is represented. In (b) inset the ΔS_{max} obtained for both applied fields is plotted as a function of $T_C^{-2/3}$.

the other for $\Delta H = 5$ T) obtained for the same J value system are in fair agreement with the ratio of the two applied field change amplitudes ($5^{-2/3}$). By substituting Eqs. (4) and (6) into Eq. (10) it is straightforward to observe that the dependency on N is simply linear, thus inducing that a material ΔS_m is maximized for denser crystal structures.

Furthermore, by considering the volume dependence of the Curie temperature given by the Bean-Rodbell model,¹⁷ first order magnetic transition systems were also simulated and studied. Surprisingly, the same overall decreasing behavior of ΔS_{max} with increasing T_C is found, as is seen in Fig. 2(a). As was already pointed out previously,¹² the shape of the simulated first-order $\Delta S_m(T)$ curves resembles the experimentally observed half bell shape. For these curves no significant changes in the FWHM values were observed between systems with different T_C . Nevertheless, the area under the curve $\Delta S_m(T)$ does not change due to the same reasoning mentioned for the second-order systems case. Moreover, in Fig. 2(b), the Curie temperature dependence of the ΔS_{max} for first-order systems with $\Delta H = 1$ and 5 T are plotted. For both cases the monotonically decreasing behavior of $\Delta S_{max}(T_C)$ is verified. As expected, the ΔS_{max} values are higher when the applied field is higher within the simulated T_C range. When comparing the ΔS_{max} normalized values for $J = 2$ first- and second-order systems [which is valid as both systems were normalized with the same factor— $Nk_B \ln(2J + 1)$], it is clear that the first-order system has much higher values than the second order ones. This difference is constant (~ 0.22) for the T_C range considered, showing that a magnetovolume coupling strong enough to promote first-order transition with small applied field changes is responsible for a significant increase in the maximum magnetic entropy change.

Finally, in Fig. 2(b) inset, these ΔS_{max} values are plotted as a function of $T_C^{-2/3}$. The linear relation of ΔS_{max} with $T_C^{-2/3}$ is again observed. The different slopes are associated with the different applied fields, in accordance with Eq. (10).

In order to compare the simulations, specifically the $T_C^{-2/3}$ dependency presented above, with experimental results, a set of data from second and first order magnetic transition systems was collected from the literature and plotted as a function of $T_C^{-2/3}$ in Figs. 3(a) and 3(b). As is clearly seen, for these second and first order magnetocaloric alloy families, ΔS_{max} follows the $T_C^{-2/3}$ dependency predicted by our calculations and modelling. The second order magnetic systems here presented were extracted from: $Gd_{1-x}Tb_xCo_2$ (for $\Delta H = 2$ T),²² $La_{2/3}(Ca_{1-x}Sr_x)_{1/3}MnO_3$ (for $\Delta H = 1$ T),²³

and $Dy(Co_{1-x}Fe_x)_2$ (for $\Delta H = 1$ T).²⁴ Also for these experimental results, different slopes are observed which probably result from their specific J and ΔH parameters, as was shown by Eq. (10).

The first order magnetic systems data were all measured with a $\Delta H = 5$ T and were extracted from: $MnFe(P_{1-x}As_x)_2$,²⁵ $Gd_5(Si_xGe_{1-x})_4$ for $x < 0.4$ (Ref. 2), and RCo_2 .²⁶ These represent a wide set of different magnetocaloric materials, thus validating the far-ranging nature of the $T_C^{-2/3}$ dependency found by our calculations. It is interesting to note that the lattice entropy contribution, which is not taken into consideration in the model, does not invalidate observing the $T_C^{-2/3}$ dependency in the studied systems. One would assume that throughout the composition ranges shown for each system in Fig. 3, this contribution is either negligible or approximately constant. This is particularly relevant in first-order systems (such as $Gd_5(Si_{1-x}Ge_x)_4$), where the lattice entropy change contribution should in principle be largely independent on composition, as long as a particular structural transition occurs. The fact that other first and second order magnetocaloric families do not show this behavior allows us to induce that such systems must have

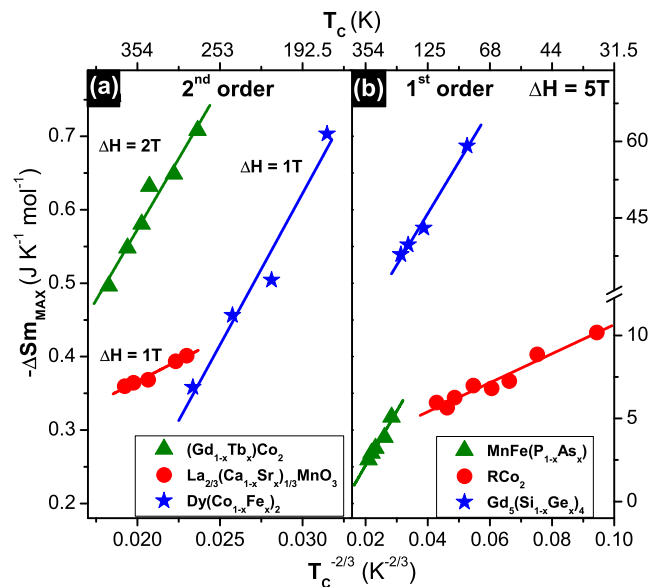


FIG. 3. (a) ΔS_{max} experimental data (in $J K^{-1} mol^{-1}$ units) as a function of $T_C^{-2/3}$ for the second order magnetic transition compounds families: $Gd_{1-x}Tb_xCo_2$ (green triangles), $La_{2/3}(Ca_{1-x}Sr_x)_{1/3}MnO_3$ (red circles), and $Dy(Co_{1-x}Fe_x)_2$ (blue stars). (b) Also $\Delta S_{max}(T_C^{-2/3})$ experimental data and normalized data for the first-order magnetic transition compounds families: $MnFe(P_{1-x}As_x)_2$ (green triangles), RCo_2 (red circles), and $Gd_5(Si_xGe_{1-x})_4$ (blue stars). The plotted lines are linear fits to the presented data.

more complex magnetocrystalline interactions than the constant magnetovolume coupling considered in these calculations. Particularly for the $\text{La}(\text{Fe}_{13-x}\text{Si}_x)$ family, the main reason for not exhibiting this behavior is most probably its complex set of minima in its total energy as a function of spin moment, which turns the transition from the paramagnetic to the ferromagnetic state into a series of consecutive transitions, as was found experimentally in Ref. 27. On the contrary, for the $\text{MnAs}_{1-x}\text{Sb}_x$ family, both the change from a first to a second order magnetic transition for low Sb concentration and the phenomenological fact that the T_C is lowered with Sb concentration induce the lowering of $\Delta\text{Sm}_{\text{max}}$ when T_C decreases, as was reported in Ref. 28.

In summary, the behavior of the magnetic entropy change of first- and second-order magnetic systems was studied as a function of Curie temperature, magnetic field change and individual spin moments. Numerical simulations, in the framework of the molecular mean field model incorporating the Bean-Rodbell magnetovolume coupling were performed. The most remarkable result was to find a $T_C^{-2/3}$ dependency of $\Delta\text{Sm}_{\text{max}}$ values in both first- and second-order systems. Such behavior was also corroborated by experimentally obtained data, collected from a wide set of first and second order magnetocaloric materials. This surprising second-order like behavior in first-order phase transition systems warrants further detailed investigation. We have shown that the magnetovolume coupling plays a decisive role on the enhancement of the magnetic entropy change compared to an increase of J , under magnetic field changes typically used in magnetic refrigeration prototypes. Therefore in the magnetocaloric materials search, efforts should be focused on optimizing magnetic coupling mechanisms as opposed to substituting magnetic ions. Finally, starting from the molecular mean field magnetization equation, an approximation of the $\Delta\text{Sm}_{\text{max}}$ as a function of T_C , H , J , and N was achieved, allowing a direct estimation of the $\Delta\text{Sm}_{\text{max}}$ for a given mean field system. Therefore we believe that this work enables a better understanding of the existing experimental MCE data and provides important guidelines for the prospection of magnetocaloric materials particularly within the room temperature range applications.

Work partially supported by the projects PTDC/CTM-NAN/115125/2009 and FEDER/POCTI 155/94 from Fundação

para a Ciência e Tecnologia (FCT), Portugal. A.M.P. and J.S.A. thank FCT for the Grant (Nos. SFRH/BPD/63150/2009 and SFRH/BPD/63942/2009).

- ¹V. K. Pecharsky and K. A. Gschneidner, *Phys. Rev. Lett.* **78**, 4494 (1997).
- ²K. A. Gschneidner, V. K. Pecharsky, and A. O. Tsokol, *Rep. Prog. Phys.* **68**, 1479 (2005).
- ³G. J. Miller, *Chem. Soc. Rev.* **35**, 799 (2006).
- ⁴A. M. Tishin and Y. I. Spichkin, *The Magnetocaloric Effect and Its Applications* (Institute of Physics Publishing, Bristol/Philadelphia, 2003).
- ⁵A. M. Pereira, E. Kamper, J. M. Moreira, U. Zeitler, J. H. Belo, C. Magen, P. A. Algarabel, L. Morellon, M. R. Ibarra, J. N. Goncalves *et al.*, *Appl. Phys. Lett.* **99**, 132510 (2011).
- ⁶V. K. Pecharsky, K. A. Gschneidner, Jr., Y. Mudryk, and D. Paudyal, *J. Magn. Magn. Mater.* **321**, 3541 (2009).
- ⁷J. H. Belo, A. M. Pereira, J. Ventura, G. N. P. Oliveira, J. P. Araujo, P. B. Tavares, L. Fernandes, P. A. Algarabel, C. Magen, L. Morellon, and M. R. Ibarra, *J. Alloys Compd.* **529**, 89–95 (2012).
- ⁸A. M. Pereira, A. M. dos Santos, C. Magen, J. B. Sousa, P. A. Algarabel, Y. Ren, C. Ritter, L. Morellon, M. R. Ibarra, and J. P. Araujo, *Appl. Phys. Lett.* **98**, 122501 (2011).
- ⁹B. G. Shen, J. R. Sun, F. X. Hu, H. W. Zhang, and Z. H. Cheng, *Adv. Mater.* **21**, 4545 (2009).
- ¹⁰K. H. J. Buschow, *Handbook of Magnetic Materials* (North-Holland, Amsterdam, 1999), Vol. 12.
- ¹¹J. S. Amaral, N. J. O. Silva, and V. S. Amaral, *Appl. Phys. Lett.* **91**, 172503 (2007).
- ¹²V. S. Amaral and J. S. Amaral, *J. Magn. Magn. Mater.* **272**, 2104 (2004).
- ¹³V. Franco, A. Conde, J. M. Romero-Enrique, and J. S. Blazquez, *J. Phys.: Condens. Matter* **20**, 1 (2008).
- ¹⁴N. A. Oliveira and P. J. Von Ranke, *Phys. Rep.* **489**, 89 (2010).
- ¹⁵J. Lyubina, M. Kuzmin, K. Nenkov, O. Gutfleisch, M. Richter, D. L. Schlager, T. A. Lograsso, and K. A. Gschneidner Jr., *Phys. Rev. B* **83**, 012403 (2011).
- ¹⁶P. Weiss, *J. Phys. Theory Appl.* **6**, 661–690 (1907).
- ¹⁷C. P. Bean and D. S. Rodbell, *Phys. Rev.* **126**, 104 (1962).
- ¹⁸J. Katriel, *Phys. Stat. Sol. (b)* **139**, 307 (1987).
- ¹⁹A. Cohen, *Rheol. Acta* **30**, 270 (1991).
- ²⁰A. S. Arrott, *J. Appl. Phys.* **103**, 07C715 (2008).
- ²¹H. E. Stanley, *Introduction to Phase Transitions and Critical Phenomena* (Clarendon, Oxford, 1971).
- ²²K. Zhou, Y. Zhuang, J. Li, J. Deng, and Q. Zhu, *Solid State Commun.* **137**, 275 (2006).
- ²³J. Mira, J. Rivas, L. E. Hueso, F. Rivadulla, and M. A. L. Quintela, *J. Appl. Phys.* **91**, 8903 (2002).
- ²⁴Z. Han, Z. Hua, D. Wang, C. Zhang, B. Gu, and Y. Du, *J. Magn. Magn. Mater.* **302**, 109 (2006).
- ²⁵O. Tegus, E. Bruck, L. Zhang, W. Dagula, K. Buschow, and F. de Boer, *Phys. B - Condens. Matter* **319**, 174 (2002).
- ²⁶N. Duc, D. Anh, and P. Brommer, *Phys. B - Condens. Matter* **319**, 1 (2002).
- ²⁷J. Lyubina, K. Nenkov, L. Schultz, and O. Gutfleisch, *Phys. Rev. Lett.* **101**, 1 (2008).
- ²⁸H. Wada and Y. Tanabe, *Appl. Phys. Lett.* **79**, 3302 (2001).